A R C H I W U M I N S T Y T U T U I N Ż Y N I E R I I L Ą D O W E J
Nr 23 ARCHIVES OF INSTITUTE OF CIVIL ENGINEERING 2017

EVALUATION OF THE CONDITION OF A SOIL-STEEL STRUCTURE BASED ON IT'S DEFORMATION[1]

Czesław MACHELSKI*, Michał MOŃKA**
*) Department of Bridges and Railways, Wrocław University of Science and Technology
**) ViaCon Polska, Rydzyna

Buried soil-steel structures are prone to deformations under its own weight, soil pressure and live loads, which results in a visible deviation from the design shape. Changes in the geometry of the circumferential shell strip are determined on the basis of the coordinates obtained using surveying techniques in this study. Any (asymmetrical) arrangement of measurement points is taken into account. The paper evaluates the effectiveness of three deformation indicators calculated during the construction and in-service stage. The change in the curvature of the shell crown constitutes the basic measure of deformation. The study indicates the feasibility of determining strain in corrugated sheets, i.e. the values identical to those obtained with use of strain gauges.

Key words: shell deformation indicator, construction, in-service stage analyses

1. SHELL DEFORMATION

After assembling a shell made of corrugated metal sheets, and upon subsequent laying of a soil backfill and constructing a road base and surface, the complexity of the shell geometry increases. Shape of the shell continues to deform during the in-service stage [1, 7], and thus substantially deviates from the design geometry defined in product catalogues. In the shell with design symmetrical geometry and a constant curvature radius R the asymmetry of circumferential strips of corrugated sheet can be observed even before backfilling, as shown in Fig. 1. This is due to the deformation resulting from the shell own weight and to the technological deviations introduced during manufacturing and assembly of corrugated sheets. The shell becomes asymmetrically deformed during backfilling as a result of soil non-homogeneity and varying degree of its compaction on both sides of the shell [3, 14], as shown in Fig. 1. The apparent lack of symmetry in a shell with regular geometry may be determined by measurements conducted using any (asymmetrical) arrangement of ABF measurement points, as shown in Fig. 1.

[1] DOI 10.21008/j.1897-4007.2017.23.17

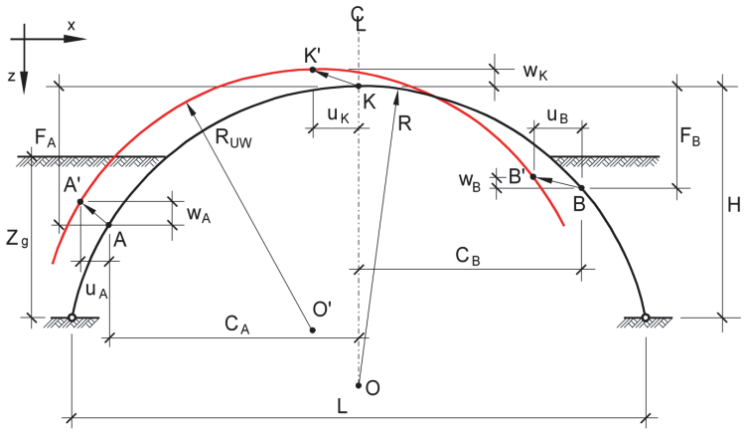

Fig. 1. Shell displacements during backfilling

This study considers the most difficult cases, i.e. structures for which there is no data recorded during construction phases. In such situation control measurement results can be related only to the design geometry of the shell given in product catalogues. This study analyses the geometrical relationships between several AKB measurement coordinates located on selected (analysed) circumferential strip of the shell [5].

2. SHELL DEFORMATION INDICATORS

Due to the considerable displacements of shell points (in the range of several dozen or, in some cases, few hundred millimetres) surveying techniques are most often used for the deformation mapping [4]. The basic and most commonly used parameter used to evaluate safety of the shell is the uplift indicator [9, 11, 13] calculated using the following equation

$$\omega = \frac{w_k}{L} 100\% < 2\% \,, \tag{1}$$

where L is the greatest horizontal dimension (span) of the shell, and w_k is the maximum uplift (upward deflection in the crown), shown in Fig. 1. Monitoring of this value involves geodetic measurement of the shell crown position during construction to compare it with the initial value (determined immediately after assembly). Maximum values of w_k usually occur when the backfill level reaches the crown, .i.e. when $z_g = H$. Thus the safety condition (1) is clearly defined and easy to control at the construction site. It is sufficient to measure its initial value and the value for $z_g = H$. Nonetheless, reliability of this indicator is disputable.

More information related to the shell deformation is obtained by analysing the narrowing indicator. Evaluation of the deformation bases on the geometry of circumferential sectors of the shell, i.e. the chords [2] with a length of $L_{AB} = 2C$. The narrowing $2u$, i.e. the decrease of the primary value L_{AB} is the sum of horizontal displacements u_A and u_B towards the shell axis (due to the substantial horizontal deformation, it is represented as $u_B - u_A$ in Fig. 1)

$$\mu = \frac{2u}{2C}100\% = \frac{u_A + u_B}{2C}100\%. \tag{2}$$

Position of measurement points A and B in relation to K, i.e. F value is critical in this case. We can thus define a function $\mu(F)$ used further in the study. In the case of closed shells, this indicator is used to evaluate the span change L (greatest horizontal dimension) as in the following equation

$$\mu_L = \frac{2u}{L}100\% < 2\%. \tag{3}$$

A reliable measure of shell deformation is the reduction of curvature in the crown [2, 5, 10], expressed as the following indicator

$$\rho = \frac{R - R_{uw}}{R_{uw}}100\% \quad . \tag{4}$$

It is determined on the basis of the curvature radius R_{uw} in the analysed shell condition and compared with e.g. design value R, as shown in Fig. 1.

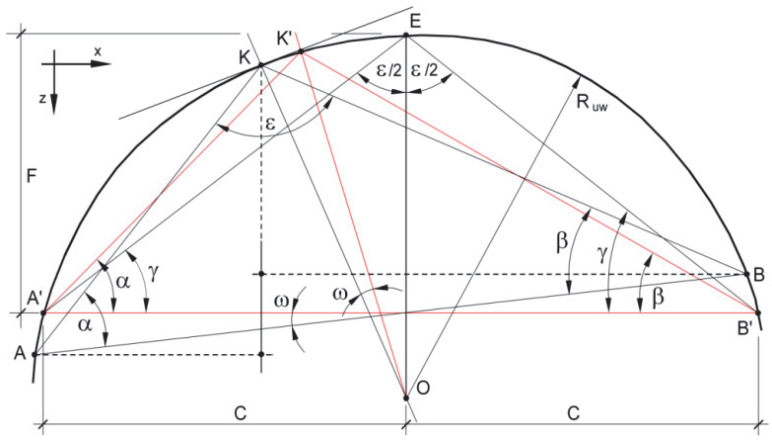

Fig. 2. Orthogonal transformation of AKB measurement points position

In practice, on the basis of the coordinates of three measurement points AKB, as shown in Figures 1 and 2, the reduction of curvature in the crown is estimated, as it is the case considered in the algorithm used in the study. The procedure uses geometric relationship between a circle and an equilateral triangle inscribed into it [5]. Thus the narrowing $2u$ and the uplift w discussed above are included in the curvature radius R_{uw}.

3. DEFORMATION INDICATORS IN THE SHELL CROWN

The values of μ and ρ determined in the crown are critical in evaluating shell safety. In the case of narrowing, if the distance between points A and B decreases, the boundary value μ_k is obtained

$$\mu_k = \lim_{F \to 0} \left(\frac{u}{C} \right) 100\% = 100 \cdot \varepsilon_d \,. \tag{5}$$

Consequently, μ_k can be directly used to determine unit strain in the circumferential direction on the bottom of the sheet corrugation ($\varepsilon_d > 0$ means compression as shown in Fig. 6). Value of ε_d results from axial force (compression) and bending moment. By summing effects of both these factors, one can obtain a maximum strain in a cross-section - at the bottom of the sheet corrugation.

In the case of the curvature reduction indicator, a boundary value is obtained

$$\rho_k = \frac{R}{f} \left(\varepsilon_d - \varepsilon_g \right) 100\% . \tag{6}$$

If ε_g stands for tension, factors ε_d and ε_g are added. Unit strains calculated in (5) and (6) can be used to create strain distribution along the height of the cross-section of the corrugated sheet, as shown in Fig. 6.

In the case of geodetic surveying μ_k is obtained by extrapolating diagram $\mu(F)$ when $F \to 0$. Fig. 4 shows the results of in situ tests conducted during construction of the structure in Rydzyna [4, 10, 11]. The shell was made of a single layer of corrugated sheets without overlays.

Table 1. Geometrical characteristics of the shell in the analysed structure

Sheet type	Shell parameters [m]		
SC 380×140×7	*L*	*H*	*R*
(Fig. 5)	17.594	5.459	13.735

Geometrical characteristics of the structure are presents in Table 1 and Fig. 3, whereas Table 2 shows a location of the measurement points. Values of F and C are subject to (minor) changes just as deformation of the shell is, as shown in Fig. 1. Due to the fact that the measurements are conducted on the bottom of the

shell corrugation, the design (given in the product catalogue) curvature radius R is corrected to the following value

$$R_d = R - \frac{f+t}{2} = 13{,}6615\,m, \tag{7}$$

and the lengths of the chords of the upper circular sectors (depending on F) are

$$C_d = \sqrt{F(2R_d - F)}\,. \tag{8}$$

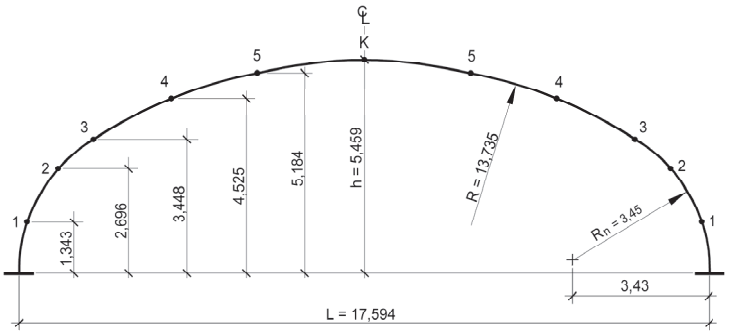

Fig. 3. Geometry of analysed shell in Rydzyna

Table 2. Measurement levels of the analysed shell

Geometrical parameters	Shell measurement lines			
	5	4	3	2
F [m]	0.275	0.934	2.011	2.763
$2C_d$ [m]	5.455	9.929	14.269	16.475

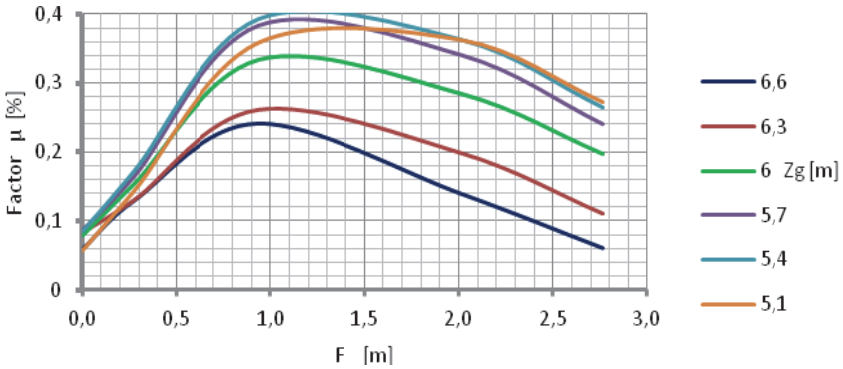

Fig. 4. Function $\mu(F,z_g)$ for the structure in Rydzyna

The diagram legend in Fig. 4 describes the backfill thickness z_g during construction, as shown in Fig. 1. As this study analyses strain gauge measurements [4], values of μ_k were calculated from (5) based on unit strains ε_d. Observed consistency of the diagrams when $F \to 0$ (generated by using two independent measurement methods) indicates the feasibility of (linear) extrapolation of $\mu(F)$ function to obtain ε_d. Low values of μ_k (even as low as 0.2% in the crown) are a common feature of these diagrams. Therefore, extrapolation of $\mu(F)$ function, when $F \to 0$, may be inaccurate.

Fig. 5 shows results of the analyses of the curvature indicator of the structure in Rydzyna. As before, values of ρ_k were calculated based on the results of tensometric measurements [4] using eq. (8). The observed correspondence of the diagrams when $F \to 0$ indicates the feasibility of the extrapolation (also linear). This follows from the shape of the diagrams and large values of ρ_k. It is critical to conduct measurements when the points A and B are located close to the crown point K, i.e. the values of F should be small.

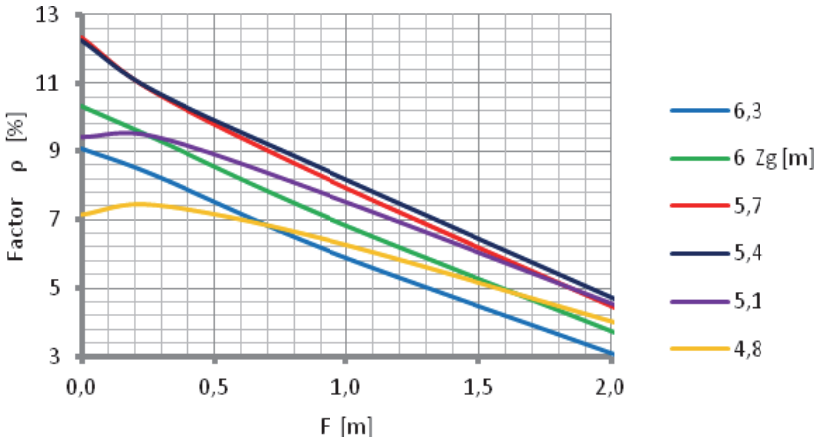

Fig. 5. Function $\rho(F,z_g)$ for the structure in Rydzyna

4. STRAINS IN CORRUGATED SHEET

If no tensometric measurements had been conducted in the structure analysed above, unit strains ε_d and ε_g would be determined on the basis of geodetic surveys by extrapolating $\mu(F)$ and $\rho(F)$ functions, as in Figures 4 and 5. Thus, the calculated value of μ_k can be used to determine the greatest unit strain ε_d. Most often it is compression on the bottom edge of the sheet when the shell had been uplifted (upward deflection). Value ρ_k can be used to determine the distribution of strain along the height of the corrugation. The type of corrugation can be described e.g. as SC $a \times f \times t$, as in Fig. 6. Assuming that cross-sections remain flat after shell deformation, strain in the axis of inertia of the shell is equal

$$\varepsilon_o = \frac{1}{2f}\left[(f-t)\varepsilon_d + (f+t)\varepsilon_g\right]. \tag{9}$$

Strain value at the top edge of the corrugation (usually unreachable during in-situ tests) can be expressed as

$$\varepsilon_G = \frac{-1}{f}\left[(f+t)\varepsilon_g - t\cdot\varepsilon_d\right]. \tag{10}$$

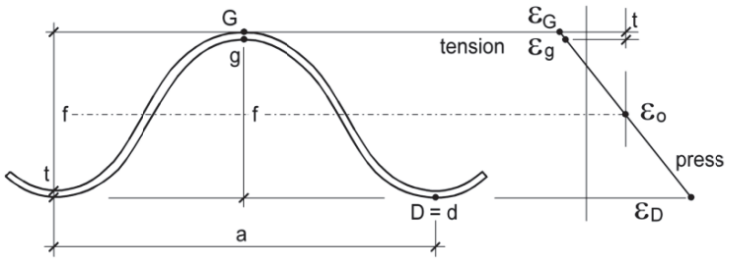

Fig. 6. Strains in a corrugated sheet cross-section

Figure 7 shows strain changes during backfilling the structure in Rydzyna. Ordinate z_g represents the backfill thickness, as shown in Fig. 1. Only strain gauge measurements [4] were used to determine the variation of strains in the circumferential direction of the shell. Strain symbols in the graph legend are described in Fig. 6. The greatest strain values are due to bending, when the backfill height reaches the crown. Bottom edge strains do not reduce rapidly when $z_g > H$ as a result of the increase of axial force in the shell.

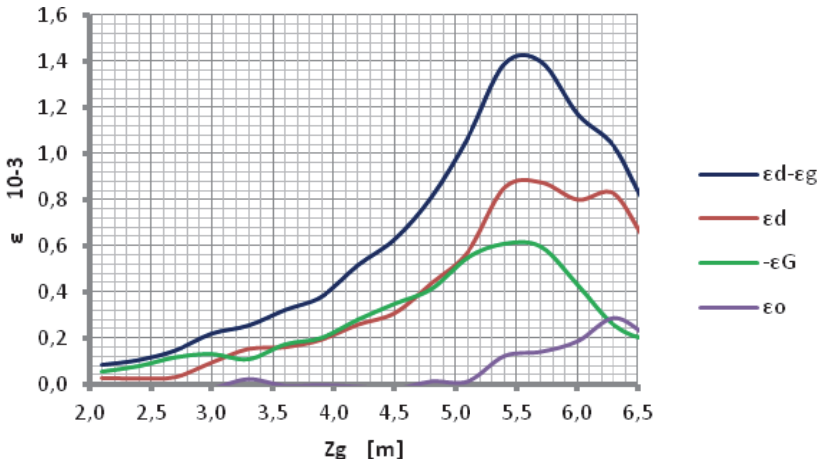

Fig. 7. Strains during the construction of the structure in Rydzyna

5. ANALYSIS OF THE UPPER SECTOR OF THE SHELL

If a large number of measurement points is used in the top sector of the circumferential strip of the shell, one can also determine values μ and ρ in points close to the crown K. Diagonal measurement lines are used for this purpose, as shown in Fig. 8 (with point 5 being the crown in the central arrangement). This can be particularly useful if shell deformation deviates from the symmetric arrangement, as in Figures 1 and 2. In the presented algorithm it is advantageous to separate the circumferential sector of the shell from the support (either direct or on a foundation) and a free choice of the shell shape (arch, pear-shaped, elliptical) but with the uniform curvature radius R in the top sector of the shell.

The example analysed below refers to the structure in Rydzyna. The measurements were conducted on October 2013, 45 months after the construction completion. The coordinates of the measurement points are summarised in Table 3, while point numbers are shown in Fig. 8. Based on the calculated coordinates, the radii of the curvature of the shell circumferential strip were calculated and presented in Fig. 9.

Table 3. Measurement point coordinates for the structure in Rydzyna

Point	X [m]	Y [m]	Z [m]
1	3.5716	1.4245	2.9992
2	3.5964	2.2733	3.6968
3	3.6243	4.4513	4.7600
4	3.6781	6.8405	5.3850
5	3.7186	9.3985	5.6322
6	3.7989	12.1333	5.3318
7	3.8702	14.4558	4.6667
8	3.9205	16.6315	3.6280
9	3.9354	17.5517	2.8315

The following measurement lines were used in the calculations:
- point arrangement **L** 3-5-6, 2-5-7 and 1-5-8;
- point arrangement **C** 4-5-6, 3-5-7, 2-5-8 and 1-5-9;
- point arrangement **R** 4-5-7, 3-5-8 and 2-5-9.

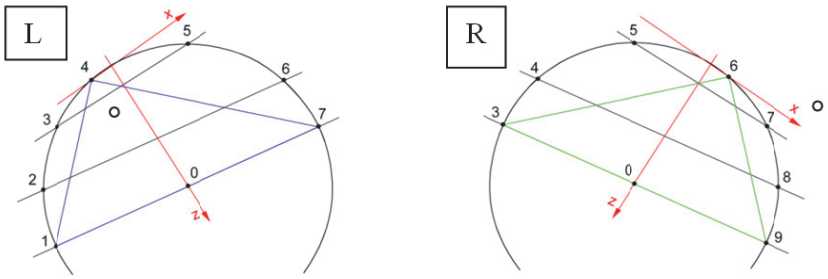

Fig. 8. Diagonal measurement lines of points adjacent to the shell crown

C is the central position of the measurement line points, whereas **L** and **R** represent arrangements shown in Fig. 8. A comparison of the graphs **L** and **R** reveals the asymmetry of the shell deformation. By extrapolating the function $R_{uw}(F)$, shown in Fig. 9, R_L, R_k and R_R were obtained. From eq. (4) the following values were calculated:

- arrangement **L** $$\rho_L = \frac{13{,}662 - 13{,}30}{13{,}30} 100\% = 2{,}72\% \quad , \tag{11}$$
- arrangement **C** $$\rho_k = \frac{13{,}662 - 12{,}15}{12{,}15} 100\% = 12{,}44\% , \tag{12}$$
- arrangement **R** $$\rho_R = \frac{13{,}662 - 12{,}90}{12{,}90} 100\% = 5{,}91\% \quad , \tag{13}$$

In this case, the control (temporary) measurement results can be related only to the design (given in product catalogue) shell geometry, thus eq. (4) assumes $R = R_d$ as in (7).

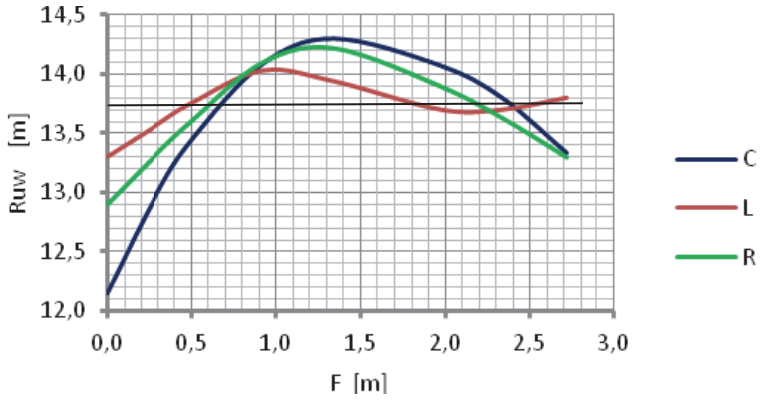

Fig. 9. Curvature radii calculated on the basis of data presented in Table 3

6. TEMPORARY SHELL DEFORMATION

Examples of structures analysed below concern the most difficult situation, when there is no data from the construction time. Results of in-situ measurements conducted during a randomly selected period of in-service stage are only used. Control measurement results can be related only to the design geometry of the shell in such situation.

This algorithm is illustrated with the evaluation of a current condition of the shells in three structures during in-service stage. Measurements were conducted with use of geodetic surveying and specifying the arrangement of points in a spatial coordinate system (as shown in Table 3). Any arrangement of points on the circumferential strip of the shell is considered. Orthogonal transformation, as shown in Fig. 2, arranges the coordinates to represent equilateral triangles inscribed in a circle with the desired curvature radius R_u.

Geometrical characteristics of the analysed structures of different types are presented in Table 4. Two of them are pipearch-shaped and one is arch-shaped, supported on a concrete foundation. Product catalogues provide values of the inner line of the circumferential strip, denoted as t. Due to the geodetic pads used for measuring, curvature radii are related to the value R_d.

Table 4 Parameters of the analysed structures

Structure	Sheet type (Fig. 5)	Shell geometry	Shell strip dimensions [m]			
			L_t	H_t	R_t	R_d
Rawicz	MP 200×50×7	VM 41	9.96	7.32	4.983	4.958
Pakówka	MP 200×50×7	VM 43	10.42	7.60	5.203	5.178
Nowa Sól	SC 380×140×7	SC 12NA	12.447	4.501	5.010	4.983

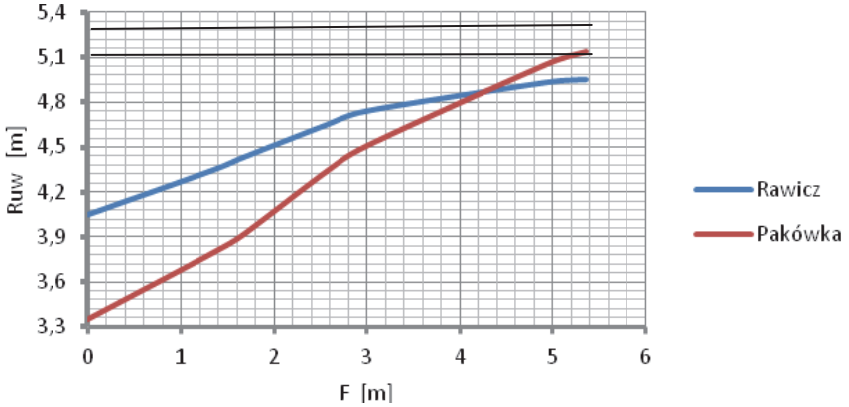

Fig. 10. Curvature radii calculated for droplet-shaped shells

Fig. 10 shows the diagrams of the curvature radii for the pipearch-shaped shells when the measurement levels were distant F_1 = 1.5 m F_2 = 2.7 m and F_3 = 5.1 m from the crown. From the diagrams there follows that the curvature radii in the crown of these shells substantially deviate from their design values. Eq. (8) and (4) can be used to determine unit strains (total values) on the bottom edge of the corrugated sheet, as shown in Fig. 6. By using the graphs shown in Fig. 10 and the value in the crown R_k (extrapolation), the following values are obtained:

– Pakówka structure

$$\varepsilon_d - \varepsilon_g = \frac{f}{R_d}\frac{R_d - R_k}{R_k} = \frac{0{,}055}{5{,}178}\frac{5{,}178 - 3{,}35}{3{,}35} = 5{,}80 \cdot 10^{-3} \quad , \tag{14}$$

– Rawicz structure

$$\varepsilon_d - \varepsilon_g = \frac{f}{R_d}\frac{R_d - R_k}{R_k} = \frac{0{,}055}{4{,}958}\frac{4{,}958 - 4{,}05}{4{,}05} = 2{,}49 \cdot 10^{-3}. \tag{15}$$

A comparison of the calculated strains and the Rydzyna structure results shown in Fig. 7 reveals large strains in the corrugated sheet in Pakówka and Rawicz structures. It should be taken into account here that there has already been a decrease of a prior extreme deformation in these shells, when $z_g = H$ (backfill level reaching the crown, as shown in Fig. 1). Therefore, strains calculated above have been reduced due to the backfilling above the crown level. The evaluation of these results should also consider that there is no data available on the initial shape of the shell after assembly, which can differ from the characteristics given in the product catalogue.

Results of calculations (narrowing values) conducted for the arch-shaped shell in Nowa Sól structure are presented in Table 5. These values are extremely low and similar to those obtained for the shell in Rydzyna, as in Fig. 4. This case also does not consider the initial condition after shell assembly.

Table 5. Calculated values of the narrowing index for the structure in Nowa Sól

Measurement level	Geometrical parameters [m]			μ [%]
	F	C_t	C_{pom}	
1	1.043	8.847	8.849	0.022
2	2.052	11.160	11.138	0.197
3	4.047	12.500	12.484	0.128

7. CONCLUSIONS

Lack of symmetry usually concerns twinned soil-steel structures built under dual carriageways [3]. The obvious deviation from symmetry appears when the backfill is inclined [3, 8, 16]. In such cases the influence of slope inclination is analysed [16] and, if it is significant, the shell is intentionally pre-deformed (inclined) to obtain symmetry in the final stage of construction. Live loads are another factor resulting in the lack of symmetry. Shell deformation (asymmetry) is observed even in the case of structures subjected to minimum variable loads, such as animal overpasses [13].

The study discusses three shell deformation indicators used to evaluate the technical condition of a structure. The most efficient, universal is the curvature indicator. It can be used to effectively control the safety of a structure, as it takes into account the geometry of the circumferential strip of a shell and a corrugated sheet. It is also important that the equations take into account the uplift and narrowing of the shell that result in strains, which makes it possible to relate the curvature indicator ρ to the grade of steel used to manufacture the sheet.

The methodology used to determine the deformations ε on the basis of shell displacement was verified in [4]. It was used to compare ε measurements obtained from tensometric. The conclusions of the work [4] demonstrate the good coherence of both independent research methods

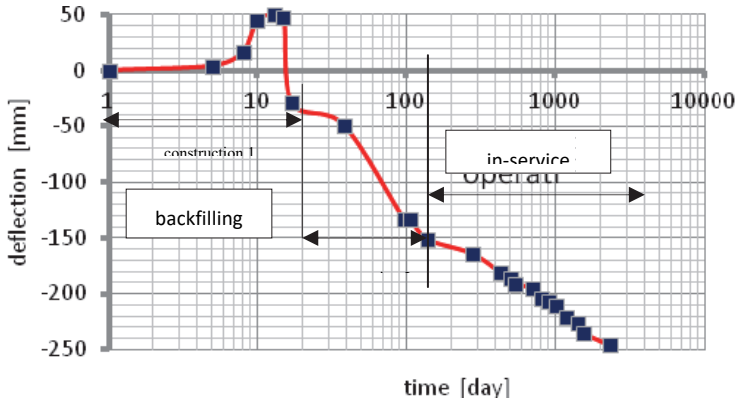

Fig. 11. Changes of uplift and downward deflection [11]

Large shell deformation indicator values can be used to monitor behaviour of a shell during in-service stage. Such example is presented in Fig. 11. In this case the phase of backfilling was extended and the shell deflection still increases during in-service stage.

LITERATURE

1. Brachman R.W.B., Elshimi T., Mak A., Moor J.D.: *Testing and Analiysis of a Deep-corrugated Large-span Box Culvert Prior to Burial.* Journal of Bridge Engineering ASCE, 2012.
2. Cowherd D.C, Corda L.J.: *Lesson learned from culvert failures and non-failures*. 89th Annual Meeting Transportation Research Board. Washington, January 11-15, 2010, p. 10-0903 (CD).
3. Kunecki B., Korusiewicz L.*: Field tests of large-span metal arch culvert during backfilling*. Roads and Bridges 12 (2013) s. 283-295.
4. Korusiewicz L.*: Verification of the method of estimating bending moments in soil-shell structures on the basis of shell deformation*. Roads and Bridges 15 (2016) s. 221-230.
5. Machelski C.: *Steel plate curvatures of soil-steel structure during construction and exploatition.* Roads and Bridges 15 (2016) s. 207-220.
6. Machelski C.: *Stiffness of railway soil-steel structures*. Studia Geotechnika et Mechanica. No. 4/2015 p. 29-36
7. Machelski C., Janusz L.: *The effects of positioning live loads over flexible soil-steel structures*. 94th Annual Meeting Transportation Research Board, Washington, 13-18 January 2015, p. 15-3359 No 620 (CD).
8. Machelski C., Janusz L.: *Deformations of Corrugated Steel Tunnel during Construction*. Underground Infrastructure of Urban Areas 3. 29-30 November 2014, p. 339-404.23
9. Machelski C., Janusz L., Czerepak A.: *Influence Functions of Shell Deflection in Soil-Steel Bridge*. Journal of Traffic and Transportation Engineering 4(2016) p. 167-175.
10. Machelski C., Janusz L., Czerepak A.: *Estimation of Stress level in the Corrugated Soil-Steel Structure Based on Deformations in the Crown*. Journal of Traffic and Transportation Engineering 4(2016) p. 186-193.
11. Machelski C. Michalski J.B. Janusz L.: *Deformation Factors of Buried Corrugated Structures*. Journal of the Transportation Research Bord. Solid Mechanics.Transportation Research Bord of Nationalals Academies, Washington D.C. 8/2009 pp. 70-75.
12. Machelski C., Michalski J. B., Janusz L.: *Parametric Analysis of Corrugated Steel Plate Structures with Maximum Spans*. 92th Annual Meeting Transportation Research Board, Washington, 13-17 January 2013, p. 13-2523 No 216.
13. Machelski C., Mońka M.: *The changes of forces and displacements of a soil-steel structure in the function of time*. Bridges. Tradition and Modernity. Wyd. Ucz. UTP Bydgoszcz 2015 s. 113-121.
14. Machelski C., Mońka M.: *Prognosis and measurements of deformation of soil-steel structure settled on steel corrugated plate foundations*. Archives of Institute of Civil Engineering. 2th European Symp. Rydzyna 23-24 April 2012, p. 147-156.
15. Machelski C., Tomala P.: *Stiffness of shells with encased concrete ribs in soil-steel bridge structures*. Archives of Institute of Civil Engineering. 2th European Symp. Rydzyna 23-24 April 2012, Wyd. Pol. Poznańskiej p. 157-166.
16. Pettersson L.: *Full Scale Tests and Structural Evaluation of Soil Steel Flexible Culverts with low Height of Cover*. Doctoral Thesis, KTH , Sweden 2007

17. Vaslestad J.: *Soil structure interaction of buried culverts*, Institutt for Geoteknikk, Norges Tekniske Hogskole, Universitetet I Trondheim,1990.
16. Czerepak A., Zouhar J.: *Deformation control during assembly and backfilling of a corrugated steel structure, Ostrava, Czech Republic*. Archives of Institute of Civil Engineering. 2th European Symp. Rydzyna 23-24 April 2012, p. 85-93.

OCENA STANU OBIEKTU GRUNTOWO-POWŁOKOWEGO NA PODSTAWIE DEFORMACJI POWŁOKI

W obiekcie gruntowo-powłokowym, w wyniku ciężaru własnego blachy falistej, parcia gruntu i obciążeń ruchomych powłoka podlega deformacji z widocznym odstępstwem od projektowego kształtu. Zmiany geometrii pasma obwodowego powłoki określa się w pracy na podstawie współrzędnych punktów uzyskanych w pomiarach geodezyjnych. Uwzględnia się przy tym dowolne (niesymetryczne) położenie punktów pomiarowych. W pracy analizuje się skuteczność trzech wskaźników deformacji powłoki obliczanych w okresie budowy lub eksploatacji obiektu. Jako podstawową miarę deformacji przyjmuje się zmianę krzywizny w kluczu powłoki a dodatkową zwężenie powłoki w pachwinach. W pracy wskazano na możliwość określania odkształceń jednostkowych w blasze falistej a więc takich jakie uzyskuje się z zastosowania tensometrii.

Słowa kluczowe: wskaźniki deformacji powłok, badania podczas budowy i eksploatacji.